JACS
JOURNAL OF THE AMERICAN CHEMICAL SOCIETY
Communication
Cite This: J. Am. Chem. Soc. 2018, 140, 12388−12391
pubs.acs.org/JACS

Synthesis and Mechanochemical Activation of Ladderene−Norbornene Block Copolymers

Jessica K. Su, John D. Feist, Jinghui Yang, Jaron A. M. Mercer, Joseph A. H. Romaniuk, Zhixing Chen, Lynette Cegelski, Noah Z. Burns, and Yan Xia*

Department of Chemistry, Stanford University, Stanford, California 94305, United States

Supporting Information

ABSTRACT: We have recently reported a polymechanophore system, polyladderene (PLDE), which dramatically transforms into polyacetylene (PA) upon mechanical stimulation. Herein, we optimized conditions to synthesize unprecedented block copolymers (BCPs) containing a force-responsive block by sequential ring-opening metathesis polymerization of different norbornenes and bromoladderene. Successful extension from PLDE to other blocks required careful timing and low temperatures to preserve the reactivity of the PLDE-appended catalyst. The PLDE-containing BCPs were sonochemically activated into visually soluble PA with a maximum absorption $\lambda \geq 600$ nm and unique absorption patterns corresponding to noncontinuous activation of ladderene units. Access to polymechanophore BCPs paves the way for new stress-responsive materials with solution and solid state self-assembly behaviors and incorporation of polymechanophores into other materials.

Mechanical force has emerged as an important stimulus to induce new reactivities that complement classical thermal and photochemical pathways and enables novel stress-responsive materials.[1] Judiciously designed mechanophores embedded in a polymer backbone may be mechanically activated to undergo constructive chemical transformations and present force-triggered functions.[2] A polymer consisting of many mechanophore repeat units is highly desired to elicit a force-response from multiple units for easier quantification of mechanochemical reactivity and potentially significant changes in polymer properties.[2e,g,3] In this regard, a monomeric mechanophore that can undergo chain-growth (ideally controlled) polymerization would significantly facilitate the synthesis of polymechanophores.

We recently reported a unique polymechanophore system, polyladderene (PLDE), that undergoes force-triggered rearrangement into polyacetylene (PA), thus transforming from an insulating polymer to a semiconducting polymer with dramatically changed material properties.[4] At relatively high degrees of activation, a mesh of insoluble, encapsulated PA nanowires was spontaneously formed. A notable feature in the design was the terminal strained cyclobutene on ladderene that allowed rapid ring-opening metathesis polymerization (ROMP). Facile and controlled polymerization of a mechanophore may enable the synthesis of unprecedented block copolymers (BCPs) containing mechanically active block(s). The rich self-assembly of BCPs in solution and bulk may lead to new force-induced behaviors and diverse nanostructures containing force-responsive domains. Functionalizable end blocks may also facilitate cross-linking of PLDE and its integration with other polymers to impart the dramatic stress-response of PLDE to diverse materials.

Herein, we report the optimized synthesis of various PLDE-containing triblock copolymers consisting of a PLDE middle block and mechanochemically inert polynorbornene (PNBE) end blocks (Figure 1). We also studied their sonochemical activation behavior using spectroscopic and chromatographic methods.

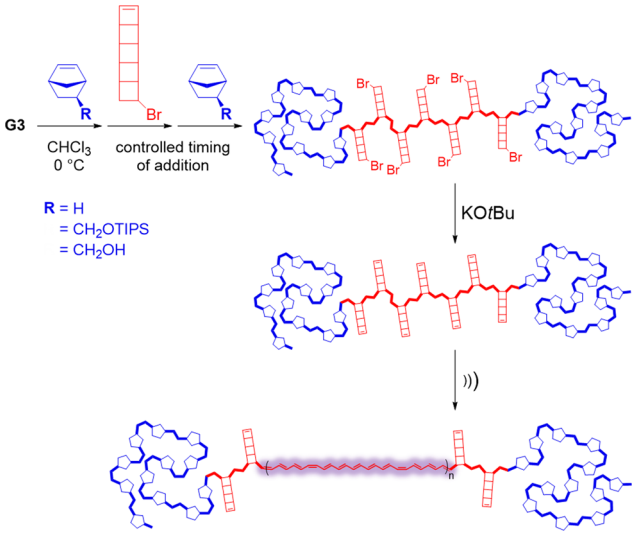

Figure 1. Synthesis and mechanoactivation of PLDE-containing triblock copolymers.

We have previously developed a chloroladderene monomer based on the synthesis of ladderane lipids.[5] HCl elimination after ROMP was required to generate a terminal cyclobutene on each ladder side chain, which allowed for continuous conjugation upon activation, but elimination resulted in some chain cleavage.[4] To facilitate the elimination, we synthesized bromoladderene (**Br-LDE**) via C−H bromination of [5]-ladderane using Groves's Mn porphyrin catalyst.[6] HX elimination from P(**Br-LDE**) was >15 times faster than from

Received: August 17, 2018
Published: September 19, 2018

DOI: 10.1021/jacs.8b08908
J. Am. Chem. Soc. 2018, 140, 12388−12391

P(**Cl-LDE**) to afford the same PLDE (*vide infra*). Thus, we used **Br-LDE** hereafter for our polymer syntheses.

We observed solvent, temperature, and concentration effects on the ROMP of **Br-LDE**. With a target degree of polymerization (DP) of 500, we first initiated ROMP using Grubbs third generation catalyst (**G3**) at $[\textbf{Br-LDE}]_0$ = 0.1 M in THF at room temperature. The resulting polymer exhibited a broad molecular weight (MW) distribution with a dispersity ($Đ$) of 1.63 (Figure S1a). Under the same conditions using chloroform as the solvent, $Đ$ was lowered to 1.41 but the formed polymer had a MW higher than the theoretical value. Running ROMP in chloroform at 0 °C and $[\textbf{Br-LDE}]_0$ = 0.1 M or increasing $[\textbf{Br-LDE}]_0$ to 0.5 M at room temperature both produced narrow-disperse P(**Br-LDE**)s with MWs close to the theoretical values (Figure S1). These results demonstrated that P(**Br-LDE**) synthesis can be controlled under optimal conditions and implied a limited stability of the P(**Br-LDE**) chain-end Ru carbene complex.

We targeted a PNBE-*b*-PLDE-*b*-PNBE structure via sequential addition of monomers to **G3**, but this seemingly straightforward synthesis proved nontrivial. We chose norbornene first as the simplest monomer. To target $\textbf{PNBE}_{500}$-*b*-$\textbf{P(Br-LDE)}_{100}$-*b*-$\textbf{PNBE}_{500}$, we added **NBE**, **Br-LDE**, and **NBE** in 5 min intervals to the ROMP solution at [M] ≥ 0.1 M in chloroform at 0 °C, and analyzed the polymerization at the end of each block by gel permeation chromatography with multiangle laser light scattering (GPC-MALLS). Compared to the first **PNBE** block, the GPC trace of diblock **PNBE**-*b*-P(**Br-LDE**) was uniformly shifted to shorter retention times, suggesting successful chain extension from **PNBE** (Figure 2). However, growing **PNBE** from the P(**Br-LDE**) chain end resulted in a trimodal MW distribution, where a noticeable fraction of the preceding diblock remained unextended (Figure 2). The unextended fraction increased when the time for the second block synthesis was prolonged to 10 min (Figure S2), suggesting partial deactivation of the PLDE chain-end Ru complex when monomer is depleting and propagation is slowed. To preserve the chain-end Ru activity, we raised the monomer concentrations to ≥0.2 M and shortened the reaction time for the P(**Br-LDE**) block from 5 to 3 min, limiting **Br-LDE** conversion to ∼75% before adding the second batch of **NBE**. The BCP synthesis was significantly improved with only a small fraction of diblock unextended and the final triblock copolymer exhibited the expected MW and low $Đ$ (Figure 2, Table S1). A consequence of adding **NBE** to P**NBE**-*b*-P(**Br-LDE**) at 75% conversion of **Br-LDE** was the formation of LDE-NBE dyads between the second and third blocks, as revealed by ^{1}H NMR spectroscopy. The allylic protons on ring-opened [4]-ladderane in LDE-LDE vs LDE-NBE dyads exhibited distinguishable chemical shifts between 2.93 and 3.29 ppm (see Figures S8−10 for detailed assignments using model polymers). We quantified that approximately 25% of LDE units were distributed in LDE-NBE dyads, in agreement with the 75% conversion of LDE at the time of NBE addition. However, the isolated P**NBE**/P(**Br-LDE**) BCPs repeatedly showed cross-linking upon storage in the solid state for several hours, a phenomenon that was never observed with P(**X-LDE**) homopolymers.

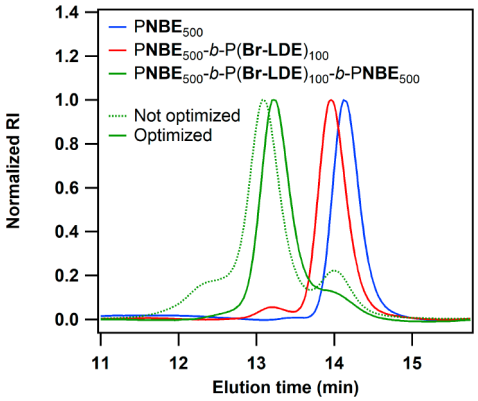

Figure 2. GPC traces of the intermediate and final blocks in the synthesis of P**NBE**-*b*-P(**Br-LDE**)-*b*-P**NBE** under optimized conditions at 0 °C.

While the nature of the cross-linking was not understood, we investigated substituted NBEs for synthesizing PLDE-containing BCPs. We selected triisopropylsilyl (TIPS) protected norbornene methanol (**NBE-TIPS**) for its stability against KO*t*Bu required in the elimination step and the possibility of being deprotected and modified postpolymerization.[7] Running ROMP at 0 °C and limiting **Br-LDE** conversion to ∼75% before adding **NBE-TIPS** for the final block resulted in P(**NBE-TIPS**)-*b*-P(**Br-LDE**)-*b*-P(**NBE-TIPS**) with the expected MW and relatively low $Đ$ despite a small fraction of the diblock copolymer remaining (Figures S3 and S4a, Tables S2 and S3). As a control, conducting ROMP at room temperature and adding **NBE-TIPS** after full **Br-LDE** conversion resulted in a significant fraction of diblock unextended (Figure S4b). NMR spectroscopy again confirmed that ∼25% of LDE units were distributed in LDE-NBE dyads under the optimized conditions (Figure S11). We also demonstrated the use of unprotected norbornene methanol (**NBE-CH$_2$OH**) to synthesize a PLDE-containing triblock copolymer with short end blocks (M_n = 21.2 kDa, $Đ$ = 1.16) (Figure S5), which can be functionalized or directly used for end-cross-linking and integration with other polymers. The BCPs synthesized using substituted NBEs remained stable under ambient conditions over several days.

We next eliminated HBr from P(**NBE-TIPS**)-*b*-P(**Br-LDE**)-*b*-P(**NBE-TIPS**) to generate a cyclobutene at the end of each ladder side chain. ^{1}H NMR spectroscopy revealed clean and complete elimination using KO*t*Bu to yield P(**NBE-TIPS**)-*b*-PLDE-*b*-P(**NBE-TIPS**) within 1 h (Figure S31), and minimal changes were observed in the GPC traces (Figure S6a). In comparison, HCl elimination from a similar BCP containing P(**Cl-LDE**) reached only 85% conversion after 16 h, slower than was observed in P(**Cl-LDE**) homopolymers, and resulted in noticeable chain cleavage under strongly basic conditions (Figure S6b) as we had previously reported.[4]

$\textbf{P(NBE-TIPS)}_{400}$-*b*-$\textbf{PLDE}_{300}$-*b*-$\textbf{P(NBE-TIPS)}_{400}$ was investigated for mechanoactivation in detail using pulsed ultrasound, a technique that applies the greatest amount of force near the center of a polymer chain.[8] A dilute solution of the polymer (0.5 μM in THF) was sonicated at 6−9 °C. After 2 min of sonication, the initially colorless polymer solution turned faintly blue; it significantly darkened with increasing sonication times, reaching dark blue after 30 min (Figure 3a). In contrast to the activation of PLDE homopolymers,[4] the activated triblock copolymer remained visually soluble throughout the course of activation. An aliquot of the solution was taken at various time points during sonication for analysis by UV−vis spectroscopy. Similar to what was observed for PLDE homopolymers, from the very beginning of sonoactiva-

DOI: 10.1021/jacs.8b08908
J. Am. Chem. Soc. 2018, 140, 12388−12391

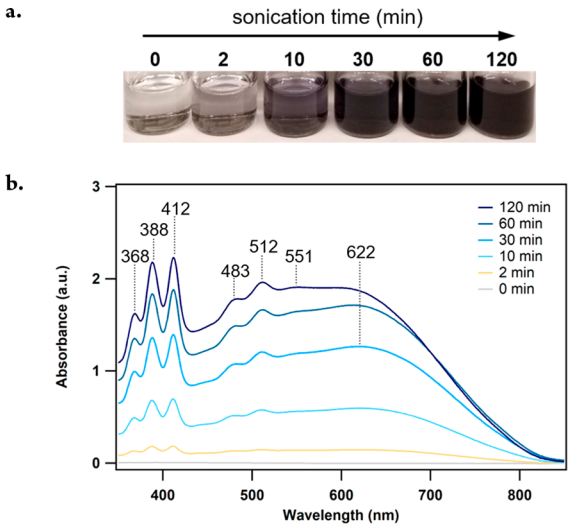

Figure 3. (a) Photograph and (b) UV−vis absorption spectra of a sonicated 0.5 μM P(**NBE-TIPS**)$_{400}$-*b*-PLDE$_{300}$-*b*-P(**NBE-TIPS**)$_{400}$ solution at different sonication times.

tion, the UV−vis spectrum showed a broad peak with an absorption maximum λ > 600 nm and onset λ = 850 nm, suggesting the formation of PA with long conjugation length (Figure 3b). Interestingly, unlike PLDE homopolymers, two distinct sets of peaks at 368, 388, and 412 nm and at 483, 512, and 551 nm were also observed. Based on Schrock and co-workers' systematic study of the absorptivity of soluble oligoenes,[9] the wavelengths and relative intensities of these peaks corresponded to the three lowest energy transitions of 7- and 13-enes, respectively. We deduced that 7- and 13-enes resulted from unzipping a single, isolated LDE and two adjacent LDE units, respectively (Figure 4). This clear optical

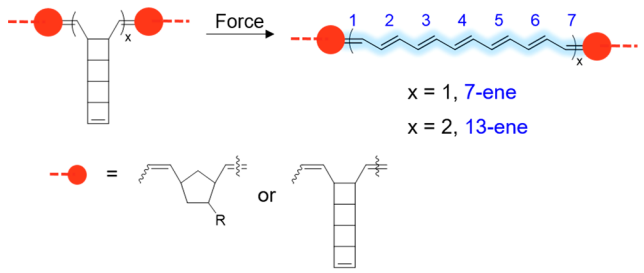

Figure 4. Mechanochemical formation of discrete oligoenes. *Trans*- and *cis*-configurations may be present in the formed oligoenes and are not specified in the figure.

readout of the continuity of mechanoactivation is a unique feature of LDE mechanochemistry due to the conjugation generated across adjacent mechanophore units. The observed discrete oligoene fractions were attributed to the presence of LDE-NBE dyads and/or noncontinuous unzipping of LDE units in the PLDE block; understanding the continuity of mechanoactivation is a focus of our future study.

We further analyzed the sonoactivation of the triblock copolymer by GPC, which was not feasible for PLDE homopolymers due to the insolubility of the activated products. The refractive index (RI) traces of the sonicated polymer at various time points showed a rapid decrease in the intensity of the original triblock copolymer peak within 10 min of sonication. Uniquely, a high MW peak was concomitantly formed without much increase in intensity for the low MW peak (Figure 5a yellow trace), which was mostly attributed to

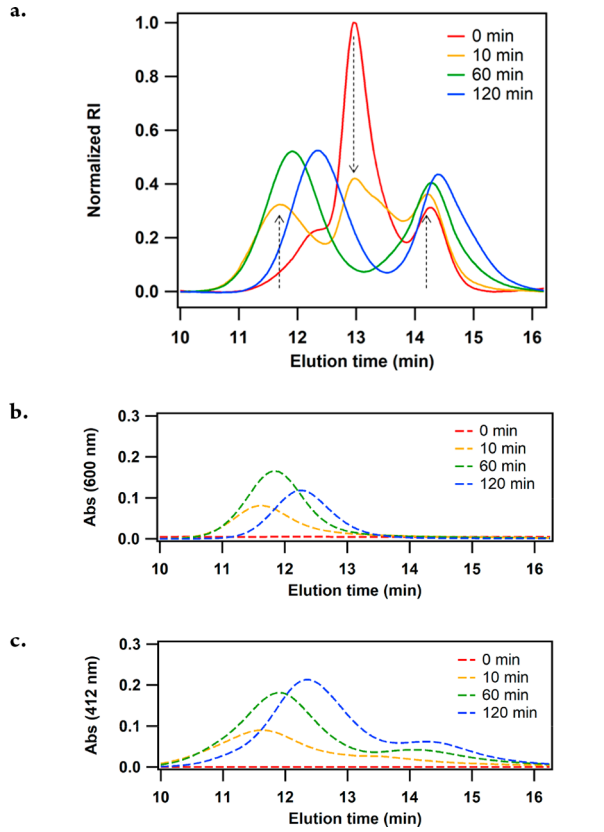

Figure 5. GPC traces of a sonicated 0.5 μM P(**NBE-TIPS**)$_{400}$-*b*-PLDE$_{300}$-*b*-P(**NBE-TIPS**)$_{400}$ solution at different sonication times based on (a) area-normalized RI, (b) absorption at 600 nm, and (c) absorption at 412 nm.

the residual diblock in the ROMP synthesis. This observation suggested that initial PLDE activation induced more nanoscale aggregation than chain cleavage. After 60 min of sonication, the original triblock copolymer peak had disappeared while the high MW peak had grown significantly, accompanied by some cleaved chains at lower MW (Figure 5a green trace). Dynamic light scattering (DLS) of the sonicated polymer solution confirmed the formation of aggregates with a hydrodynamic diameter of 50−60 nm during the course of sonoactivation (Figure S12). Atomic force microscopy (AFM) of the sonicated solution also revealed the formation of spherical nanostructures (Figure S13). Further, interestingly, using a UV−vis detector set to 600 nm (approximately the absorption maximum of the generated PA), we located the 600 nm absorption to be entirely from the high MW peak (Figure 5b), indicating that the mechanochemically generated PA had fully aggregated. The low MW peak was absent of 600 nm absorption, suggesting that this population of chains contained low or noncontinuous LDE activation. Setting the UV−vis detector to 412 nm (the absorption maximum of 7-ene), we observed relatively strong absorption in the aggregate peak and weak absorption in the low MW peak (Figure 5c), affirming the relatively low amount of noncontinuous activation in the low MW peak. After 2 h of sonication, both high and low MW peaks shifted to longer elution times (Figure 5a blue trace), indicating mechanochemical chain cleavage. Using a control

DOI: 10.1021/jacs.8b08908
J. Am. Chem. Soc. 2018, 140, 12388−12391

sample, we also confirmed that the residual diblock copolymer from the triblock synthesis only experienced a small extent of activation and contributed negligibly to the observed absorption under the sonication conditions (Figures S7 and S15).

Nanoscale aggregation strongly suppressed signals from the formed PA and remaining PLDE in solution NMR spectroscopy, so we used solid-state ^{13}C NMR spectroscopy to analyze the activated polymer. Relative to the PNBE sp^2 carbon signal centered at 134 ppm, a diminution in the PLDE sp^2 carbon at 141 ppm was observed along with an increase in upfield contributions distinct from the PNBE sp^2 carbons. Direct subtraction of PLDE and PNBE spectra from the activated polymer spectrum revealed two carbon resonances at 136 and 129 ppm corresponding to *trans*- and *cis*-PA in a ~2:1 ratio (Figure S16). The signal for *cis*-PA had not been observed previously in our activated homo-PLDE.[4] We therefore suspected the presently observed *cis*-configuration to have arisen from the generated oligoenes in the BCP, which did not undergo a mechanochemical *cis*−*trans* isomerization as was observed in extended PA.[4] We hypothesize a higher barrier for sonochemical *cis*−*trans* isomerization in oligoenes than PA.[10] Based on the spectral analysis of the total generated sp^2 carbon signals, including quantitative cross-polarization array measurements of samples before and after sonication, we determined that 36% of LDE units in P(**NBE-TIPS**)$_{400}$-*b*-PLDE$_{300}$-*b*-P(**NBE-TIPS**)$_{400}$ was activated to PA and oligoenes after 120 min of sonication. The incomplete activation may be ascribed to several factors: the presence of residual unactivated diblock copolymer, the strong aggregation of activated LDE units shielding proximal intact LDE units inside the aggregates from elongation, and nonselective chain cleavage due to the high shearing forces generated in sonication.

In conclusion, we have demonstrated successful syntheses of the first BCPs containing a mechanically active PLDE block via sequential monomer additions using ROMP under optimized conditions to preserve the reactivity of the PLDE chain-end Ru complex. Sonoactivation of PNBE-*b*-PLDE-*b*-PNBE yielded visually soluble but nanoscale aggregating PA. The ability to synthesize BCPs containing mechanically active block(s) enables the preparation of various stress-responsive materials. Exploration of solid-state activation using PLDE-containing BCPs is underway.

■ ASSOCIATED CONTENT

Supporting Information

The Supporting Information is available free of charge on the ACS Publications website at DOI: 10.1021/jacs.8b08908.

Synthetic procedures, quantification method of homo- vs cross-propagation dyads, and additional GPC traces and NMR spectra (PDF)

■ AUTHOR INFORMATION

Corresponding Author

*yanx@stanford.edu

ORCID

Zhixing Chen: 0000-0001-5962-7359
Lynette Cegelski: 0000-0002-0978-1814
Noah Z. Burns: 0000-0003-1064-4507
Yan Xia: 0000-0002-5298-748X

Notes

The authors declare no competing financial interest.

■ ACKNOWLEDGMENTS

This work was supported by the U.S. Army Research Office under grant number W911NF-15-1-0525. Part of this work was performed at the Stanford Nano Shared Facilities (SNSF), supported by the National Science Foundation under award ECCS-1542152. J.A.M.M. thanks the National Science Foundation for a graduate fellowship. We thank Lily Chen for initial exploration of BCP synthesis.

■ REFERENCES

(1) For recent reviews, see: (a) Li, J.; Nagamani, C.; Moore, J. S. *Acc. Chem. Res.* **2015**, *48*, 2181−2190. (b) Brown, C. L.; Craig, S. L. *Chem. Sci.* **2015**, *6*, 2158−2165. (c) *Polymer Mechanochemistry*; Boulatov, R., Ed.; Springer: Berlin, 2015.

(2) (a) Hickenboth, C. R.; Moore, J. S.; White, S. R.; Sottos, N. R.; Baudry, J.; Wilson, S. R. *Nature* **2007**, *446*, 423−427. (b) Potisek, S. L.; Davis, D. A.; Sottos, N. R.; White, S. R.; Moore, J. S. *J. Am. Chem. Soc.* **2007**, *129*, 13808−13809. (c) Davis, D. A.; Hamilton, A.; Yang, J.; Cremar, L. D.; Van Gough, D.; Potisek, S. L.; Ong, M. T.; Braun, P. V.; Martinez, T. J.; White, S. R.; Moore, J. S.; Sottos, N. R. *Nature* **2009**, *459*, 68−72. (d) Piermattei, A.; Karthikeyan, S.; Sijbesma, R. P. *Nat. Chem.* **2009**, *1*, 133−137. (e) Lenhardt, J. M.; Ong, M. T.; Choe, R.; Evenhuis, C. R.; Martinez, T. J.; Craig, S. L. *Science* **2010**, *329*, 1057−1060. (f) Chen, Y.; Spiering, A. J.; Karthikeyan, S.; Peters, G. W.; Meijer, E. W.; Sijbesma, R. P. *Nat. Chem.* **2012**, *4*, 559−562. (g) Ramirez, A. L.; Kean, Z. S.; Orlicki, J. A.; Champhekar, M.; Elsakr, S. M.; Krause, W. E.; Craig, S. L. *Nat. Chem.* **2013**, *5*, 757−761. (h) Larsen, M. B.; Boydston, A. J. *J. Am. Chem. Soc.* **2013**, *135*, 8189−8192. (i) Diesendruck, C. E.; Peterson, G. I.; Kulik, H. J.; Kaitz, J. A.; Mar, B. D.; May, P. A.; White, S. R.; Martinez, T. J.; Boydston, A. J.; Moore, J. S. *Nat. Chem.* **2014**, *6*, 623−628. (j) Imato, K.; Kanehara, T.; Ohishi, T.; Nishihara, M.; Yajima, H.; Ito, M.; Takahara, A.; Otsuka, H. *ACS Macro Lett.* **2015**, *4*, 1307−1311. (k) Robb, M. J.; Moore, J. S. *J. Am. Chem. Soc.* **2015**, *137*, 10946−10949. (l) Wang, J.; Kouznetsova, T. B.; Niu, Z.; Ong, M. T.; Klukovich, H. M.; Rheingold, A. L.; Martinez, T. J.; Craig, S. L. *Nat. Chem.* **2015**, *7*, 323−327. (m) Di Giannantonio, M.; Ayer, M. A.; Verde-Sesto, E.; Lattuada, M.; Weder, C.; Fromm, K. M. *Angew. Chem., Int. Ed.* **2018**, *57*, 11445−11450.

(3) (a) Lenhardt, J. M.; Black, A. L.; Craig, S. L. *J. Am. Chem. Soc.* **2009**, *131*, 10818−10819. (b) Lenhardt, J. M.; Ogle, J. W.; Ong, M. T.; Choe, R.; Martinez, T. J.; Craig, S. L. *J. Am. Chem. Soc.* **2011**, *133*, 3222−3225. (c) Kean, Z. S.; Niu, Z.; Hewage, G. B.; Rheingold, A. L.; Craig, S. L. *J. Am. Chem. Soc.* **2013**, *135*, 13598−13604. (d) Wang, J.; Piskun, I.; Craig, S. L. *ACS Macro Lett.* **2015**, *4*, 834−837. (e) Zhang, H.; Li, X.; Lin, Y.; Gao, F.; Tang, Z.; Su, P.; Zhang, W.; Xu, Y.; Weng, W.; Boulatov, R. *Nat. Commun.* **2017**, *8*, 1147. (f) Bowser, B. H.; Craig, S. L. *Polym. Chem.* **2018**, *9*, 3583−3593.

(4) Chen, Z.; Mercer, J. A. M.; Zhu, X.; Romaniuk, J. A. H.; Pfattner, R.; Cegelski, L.; Martinez, T. J.; Burns, N. Z.; Xia, Y. *Science* **2017**, *357*, 475−479.

(5) Mercer, J. A. M.; Cohen, C. M.; Shuken, S. R.; Wagner, A. M.; Smith, M. W.; Moss, F. R.; Smith, M. D.; Vahala, R.; Gonzalez-Martinez, A.; Boxer, S. G.; Burns, N. Z. *J. Am. Chem. Soc.* **2016**, *138*, 15845−15848.

(6) Liu, W.; Groves, J. T. *J. Am. Chem. Soc.* **2010**, *132*, 12847−12849.

(7) Sun, G.; Hentschel, J.; Guan, Z. *ACS Macro Lett.* **2012**, *1*, 585−588.

(8) May, P. A.; Moore, J. S. *Chem. Soc. Rev.* **2013**, *42*, 7497−7506.

(9) Knoll, K.; Schrock, R. R. *J. Am. Chem. Soc.* **1989**, *111*, 7989−8004.

(10) Wyman, G. M. *Chem. Rev.* **1955**, *55*, 625−657.

DOI: 10.1021/jacs.8b08908
J. Am. Chem. Soc. 2018, 140, 12388−12391